



## Observations of extended VHE gamma-ray emission from MSH 15-52 with CANGAROO-III

T.NAKAMORI<sup>1</sup>, G.V.BICKNELL<sup>2</sup>, R.W.CLAY<sup>3</sup>, P.G.EDWARDS<sup>4</sup>, R.ENOMOTO<sup>5</sup>, S.GUNJI<sup>6</sup>, S.HARA<sup>7</sup>, T.HARA<sup>8</sup>, T.HATTORI<sup>9</sup>, S.HAYASHI<sup>10</sup>, Y.HIGASHI<sup>1</sup>, Y.HIRAI<sup>11</sup>, K.INOUE<sup>6</sup>, C.ITOH<sup>7</sup>, S.KABUKI<sup>1</sup>, F.KAJINO<sup>10</sup>, H.KATAGIRI<sup>12</sup>, A.KAWACHI<sup>9</sup>, T.KIFUNE<sup>5</sup>, R.KIUCHI<sup>5</sup>, H.KUBO<sup>1</sup>, J.KUSHIDA<sup>9</sup>, Y.MATSUBARA<sup>13</sup>, T.MIZUKAMI<sup>1</sup>, Y.MIZUMOTO<sup>14</sup>, R.MIZUNIWA<sup>9</sup>, M.MORI<sup>5</sup>, H.MURASHI<sup>15</sup>, Y.MURAKI<sup>13</sup>, T.NAITO<sup>8</sup>, S.NAKANO<sup>1</sup>, D.NISHIDA<sup>1</sup>, K.NISHIJIMA<sup>9</sup>, M.OHISHI<sup>5</sup>, Y.SAKAMOTO<sup>9</sup>, A.SEKI<sup>9</sup>, V.STAMATESCU<sup>3</sup>, T.SUZUKI<sup>11</sup>, D.L.SWABY<sup>3</sup>, T.TANIMORI<sup>1</sup>, G.THORNTON<sup>3</sup>, F.TOKANAI<sup>6</sup>, K.TSUCHIYA<sup>1</sup>, S.WATANABE<sup>1</sup>, Y.YAMADA<sup>10</sup>, E.YAMAZAKI<sup>9</sup>, S.YANAGITA<sup>11</sup>, T.YOSHIDA<sup>11</sup>, T.YOSHIKOSHI<sup>5</sup>, Y.YUKAWA<sup>5</sup>

<sup>1</sup> Department of Physics, Kyoto University, Sakyo-ku, Kyoto 606-8502, Japan

<sup>2</sup> Research School of Astronomy and Astrophysics, Australian National University, ACT 2611, Australia

<sup>3</sup> School of Chemistry and Physics, University of Adelaide, SA 5005, Australia

<sup>4</sup> Narrabri Observatory of the Australia Telescope National Facility, CSIRO, Epping, NSW 2121, Australia

<sup>5</sup> Institute for Cosmic Ray Research, University of Tokyo, Kashiwa, Chiba 277-8582, Japan

<sup>6</sup> Department of Physics, Yamagata University, Yamagata, Yamagata 990-8560, Japan

<sup>7</sup> Ibaraki Prefectural University of Health Sciences, Ami, Ibaraki 300-0394, Japan

<sup>8</sup> Faculty of Management Information, Yamanashi Gakuin University, Kofu, Yamanashi 400-8575, Japan

<sup>9</sup> Department of Physics, Tokai University, Hiratsuka, Kanagawa 259-1292, Japan

<sup>10</sup> Department of Physics, Konan University, Kobe, Hyogo 658-8501, Japan

<sup>11</sup> Faculty of Science, Ibaraki University, Mito, Ibaraki 310-8512, Japan

<sup>12</sup> Department of Physical Science, Hiroshima University, Higashi-Hiroshima, Hiroshima 739-8526, Japan

<sup>13</sup> Solar-Terrestrial Environment Laboratory, Nagoya University, Nagoya, Aichi 464-8602, Japan

<sup>14</sup> National Astronomical Observatory of Japan, Mitaka, Tokyo 181-8588, Japan

<sup>15</sup> School of Allied Health Sciences, Kitasato University, Sagami-hara, Kanagawa 228-8555, Japan

nakamori@cr.scphys.kyoto-u.ac.jp

**Abstract:** The gamma-ray pulsar PSR B1509-58, surrounded by the supernova remnant MSH15-52, was expected to be a Very High Energy gamma-ray source. The CANGAROO-I 3.8 m telescope reported a marginal detection of VHE gamma-rays above 1.9 TeV and recently H.E.S.S. detected an extended signal along with the pulsar jets, from sub-TeV to tens of TeV. We observed MSH15-52 using CANGAROO-III imaging atmospheric Cherenkov telescope array located in South Australia, from April to June in 2006. We detected gamma-rays above 860 GeV with 7 sigma level during a total exposure of 48.4 hours. Obtained differential flux of VHE gamma-ray is consistent with that of H.E.S.S., and its morphology shows an extended emission compared to our Point Spread Function.

## Introduction

PSR B1509-58 was detected in the radio supernova remnant MSH15-52(G320.4-1.2). It was detected initially as a 150-ms X-ray pulsar by Einstein satellite[23] and subsequently at radio frequencies[18] and soft  $\gamma$ -rays by

COMPTEL[17]. EGRET, however, didn't detect pulsation at hard  $\gamma$ -ray band[17]. One of the most energetic young pulsar PSR B1509-58 has the highest period derivative  $\dot{P} = 1.5 \times 10^{-12}$ , the characteristic age  $\tau = 1700$  yr, the relatively high spin-down luminosity  $\dot{E} = 1.8 \times 10^{37}$  erg/s and the large dipole surface magnetic field

$B = 1.5 \times 10^{13}$  G [14]. The radio morphology of MSH15-52 consists of the southeast and northwest shells. The latter spatially coincided with the H II region, RCW89[21], and [11] concluded that MSH 15-52, PSR B1509-58 and RCW89 were associated systems and the distance to be  $5.2 \pm 1.4$  kpc by precise radio and X-ray data. Outflow jets, similar to the Crab or the Vela pulsar, were observed by ASCA [24], ROSAT[25] or Chandra [12] and the one towards northwest was terminated at RCW89. Detailed Chandra observation revealed sequential heating of RCW89 by the precessing pulsar jet[26]. Ginga satellite discovered a single power-law emission up to 20 keV with a photon index of  $\sim 2$ , indicating synchrotron emission and the existence of accelerated electrons[2]. BeppoSAX detected nonthermal emission from 1 keV up to 200 keV with  $\Gamma = 2.08 \pm 0.01$  [19], while the recent observations of INTEGRAL satellite found a significant spectral cut off at  $\sim 160$  keV[10] which strongly constrained maximum energies of electrons in the diffuse PWN. Since high energy electrons existed, very high energy  $\gamma$ -ray emission was expected by inverse Compton(IC) scattering with cosmic microwave background(CMB) photons[5] and CANGAROO-I indicate a possible VHE  $\gamma$ -ray detection of  $\sim 10\%$  Crab flux above 1.9 TeV, assuming the spectral index of 2.5[22]. After that H.E.S.S. reported an extended VHE  $\gamma$ -ray emission along with the pulsar jet. It showed good coincidence with the X-ray morphology, indicating inverse Compton scattering of relativistic electrons. IC radiation with CMB did not dominantly account for TeV flux, which indicated contributions of IR photons or starlight on the IC process[1]. Here we report the preliminary result of CANGAROO-III observations.

## Observations and analysis

CANGAROO-III is an array of four imaging atmospheric Cherenkov telescopes (IACTs), located at Woomera, South Australia ( $136^{\circ}47'E$ ,  $31^{\circ}06'S$ , 160m a.s.l.). Each telescope has a 10m-diameter reflector which consists of 114 segmented FRP spherical mirrors[15] mounted on a parabolic frame. The telescopes are placed at the corner of a diamond shape with an interval of 100 m[6]. The oldest telescope T1, which was the CANGAROO-

II, is not used due to its smaller FOV and higher energy threshold. Imaging camera systems on the used three telescopes (T2, T3 and T4) are identical and their FOV are  $4.0^{\circ}$  with 427 PMTs for each, given in Kabuki et al.(2003) in detail.

The observations were made from April to June in 2006. The tracking positions were offset by  $\pm 0.5^{\circ}$  from PSR B1509-58 in declination or in right ascension and changed every twenty minutes for the purpose of suppressing local effects on the camera plane by 4.1 and 4.5 magnitude bright stars. Before data recording, individually telescopes were required more than four pixels receiving over 7.6 photoelectrons and the global trigger system decided the coincidence of any two of the three telescopes[20]. We rejected data taken in bad weather conditions from analysis and finally the selected data were taken at a mean zenith angle of  $30.1^{\circ}$  and a typical trigger rate of 3-fold coincidence was 12 Hz. A total live time was 48.4 hours.

The basic analysis procedures were described in the reference[7] and [8]. After the image cleaning, the Hillas parameters were calculated for each images. We discarded events when any hits with  $\geq 15$ th brightest ADC values were in the outermost layer, in order not only to improve energy resolutions but also to avoid the deformation of the Hillas parameters, especially of *length*, which causes worse separation between  $\gamma$ -ray incident events and hadronic ones. The orientation angles were determined by minimizing sum of squared *WIDTHs* with a constraint by predicted *DISTANCE* values. After that we applied the Fisher Discriminant (FD) method[9] with a multi-parameter set of  $\vec{P} = (W2, W3, W4, L2, L3, L4)$ , where *W* and *L* are energy corrected *WIDTH* and *LENGTH*, and suffixes represent the telescope IDs. For the background study we selected a ring region around the target,  $0.2 \leq \theta^2 \leq 0.5$  [ $\text{deg}^2$ ], then we obtained FD distributions of background( $F_{bg}$ ) and Monte-Carlo  $\gamma$ -rays( $F_{\gamma}$ ). Reflectivities of each dishes used in the simulations are monitored every month by muon rings analysis of another data taken by the individual telescopes. We obtained relative of the light collection as (0.56, 0.61, 0.62) for T2, T3 and T4 respectively. Finally we could fit the FD distributions with a liner combination of these two components, that is, one parameter fitting; observed FD distribution  $F$  should be represented as

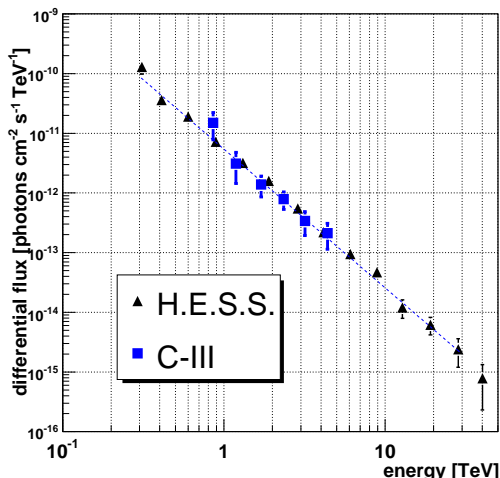


Figure 1: Differential TeV flux obtained by CANGAROO-III (blue squares), compared with those of H.E.S.S. (black triangles). Dotted line represents the best fit of single power law.

$F = \alpha F_{\gamma} + (1 - \alpha) F_{bg}$ . This analysis method was checked by an analysis of the Crab nebula data taken in December 2005.

## Results

The obtained morphology of  $\gamma$ -ray like events is shown in Fig. 2. We detected  $427 \pm 63$  excess events with a point source assumption ( $\theta^2 < 0.06$ ) and the total number of the excess within a circle of  $\theta^2 < 0.1$  is  $582 \pm 77$ , corresponding to the whole X-ray nebula, encircling the whole pulsar jet structures. Fig. 1 presents reconstructed VHE  $\gamma$ -ray spectrum. Typical flux at 2.35 TeV is  $(7.4 \pm 1.3_{\text{stat}}) \times 10^{-12} \text{ cm}^{-2} \text{ s}^{-1} \text{ TeV}^{-1}$  with a photon index of  $2.32 \pm 0.42_{\text{stat}}$ . Systematic errors are under study.

## Discussion

Our result shows the stability TeV emission between H.E.S.S. observation in 2004 and ours in 2006, which is also consistent with the steady X-ray emission from the diffuse PWN for decades [4].

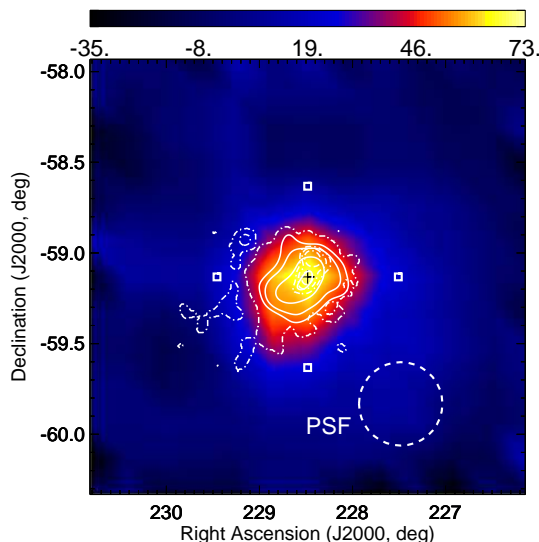


Figure 2: Morphology of TeV emission. Positions of the pulsar and tracking are indicated by a cross and squares. Our PSF [27] is also shown in the bottom of the panel. Solid contour and dot-line contours represent H.E.S.S. and ROSAT results, respectively.

Figure 3 shows the multi wavelength spectrum of diffuse PWN [11] of PSR B1509-58. These data points except this work were derived from H.E.S.S. [1] for TeV, INTEGRAL [10] for hard X-ray, Chandra [11] for soft X-ray and ATCA for radio band. Arrows in the radio band show whole emission from MSH 15-52 or RCW 89 [5] [3] so we treated them as ULs on the PWN we concerned. We reproduced this SED with an assumption of a population of nonthermal electrons as a broken power-law and uniform magnetic field  $B$ . COMPTEL and EGRET data points were omitted from fitting because of the possible contamination of the radiation from the pulsar itself. The best fit answer will be shown in the conference, and we are going to refer to the decided parameters;  $B$ , electron maximum energy  $E_{max}$  and the age of the PWN.

## Acknowledgments

This work was supported by a Grant-in-Aid for Scientific Research by the Japan Ministry of Ed-

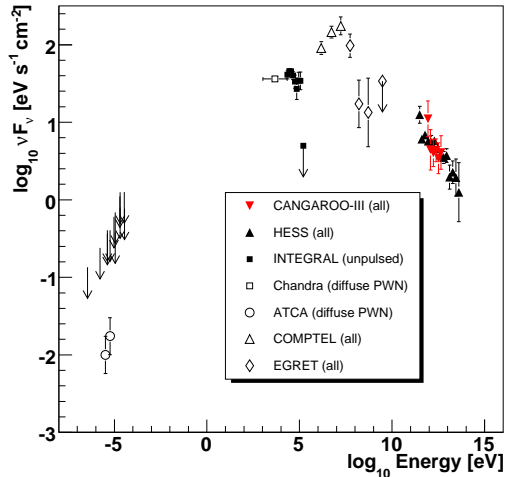


Figure 3: Spectral energy distribution. Note that COMPTEL and EGRET data points [17] contains pulsed emissions, and upper limits at radio frequencies represents emissions from whole remnant where most of them are from RCW 89. The references of data are given in the text.

education, Culture, Sports, Science and Technology, the Australian Research Council, JSPS Research Fellowships, and Inter-University Researches Program by the Institute for Cosmic Ray Research. The work is also supported by the grants-in-aid for a 21st century center of excellence program “Center for Diversity and Universality in Physics”. We thank the Defense Support Center Woomera and BAE systems. The author and Y.H. were supported by Research Fellowship of Japan Society of Promotion of Science.

## References

[1] Aharonian, F. A. et al., *A&A*, 435, L17, 2005  
 [2] Asaoka, I. & Koyama, K., *PASJ*, 42, 625, 1990  
 [3] Bednarek, W. & Bartosik, M., *A&A*, 405, 689, 2003  
 [4] Delaney, T., et al., *ApJ*, 640, 929, 2006  
 [5] du Plessis, I, et al., *ApJ*, 453, 746, 1995  
 [6] Enomoto, R., et al., *Astropart. Phys.* 16, 235, 2002

[7] Enomoto, R., et al., *ApJ*, 638, 397, 2006  
 [8] Enomoto, R., et al., *ApJ*, 652, 1268, 2006  
 [9] Fisher, R. A., *Annals of Eugenics*, 7, 179, 1936  
 [10] Forot, M., et al., *ApJ*, 651, L45, 2006  
 [11] Gaensler, B. M., et al., *MNRAS*, 305, 724, 1999  
 [12] Gaensler, B. M., et al., *ApJ*, 569, 878, 2001  
 [13] Kabuki, S., et al., *Nucl. Inst. Meth.*, A500, 318, 2003  
 [14] Kaspi, V. M., et al., *ApJ*, 422, L83, 1994  
 [15] Kawachi, A., et al., *Astropart. Phys.*, 14, 261, 2001  
 [16] Khélifi, B. et al., in *Proc. of the 29th ICRC (Pune)*, 4, 127  
 [17] Kuiper, L., et al., *A&A*, 351, 119, 1999  
 [18] Manchester, R. N., et al., *ApJ*, 262, L31, 1982  
 [19] Mineo, T., et al., *A&A*, 380, 695, 2001  
 [20] Nishijima, K., et al., in *Proc. of the 29th ICRC (Pune)*, OG2.7, 105, 2005  
 [21] Rodgers, A. W. et al., *MNRAS*, 121, 103, 1960  
 [22] Sako, T., et al., *ApJ*, 537, 422, 2000  
 [23] Seward, F. D. & Harden, F. R., *ApJ*, 256, L45, 1982  
 [24] Tamura, K., et al., *PASJ*, 48, L33, 1996  
 [25] Trussini, E., et al., *A&A*, 306, 581, 1996  
 [26] Yatsu, Y., et al., *ApJ*, 631, 312, 2005  
 [27] Yoshikoshi, T., et al., in *Proc. of the 29th ICRC (Pune)*, OG2.7, 315, 2005